Published in final edited form as:
Exp Biol Med (Maywood). 2012 September 1; 237(9): 1068–1083. doi:10.1258/ebm.2012.012052.

Elevated extracellular glucose and uncontrolled type 1 diabetes enhance NFAT5 signaling and disrupt the transverse tubular network in mouse skeletal muscle

Erick O Hernández-Ochoa[1], **Patrick Robison**[1], **Minerva Contreras**[1], **Tiansheng Shen**[1], **Zhiyong Zhao**[2], and **Martin F Schneider**[1]

[1]Department of Biochemistry and Molecular Biology, University of Maryland, School of Medicine, Baltimore, MD 21201, USA

[2]Department of Obstetrics, Gynecology, and Reproductive Sciences, University of Maryland, School of Medicine, Baltimore, MD 21201, USA

Abstract

The transcription factor nuclear factor of activated T-cells 5 (NFAT5) is a key protector from hypertonic stress in the kidney, but its role in skeletal muscle is unexamined. Here, we evaluate the effects of glucose hypertonicity and hyperglycemia on endogenous NFAT5 activity, transverse tubular system morphology and Ca^{2+} signaling in adult murine skeletal muscle fibers. We found that exposure to elevated glucose (25–50 mmol/L) increased NFAT5 expression and nuclear translocation, and NFAT-driven transcriptional activity. These effects were insensitive to the inhibition of calcineurin A, but sensitive to both p38a mitogen-activated protein kinases and phosphoinositide 3-kinase-related kinase inhibition. Fibers exposed to elevated glucose exhibited disrupted transverse tubular morphology, characterized by swollen transverse tubules and an increase in longitudinal connections between adjacent transverse tubules. Ca^{2+} transients elicited by a single, brief electric field stimuli were increased in amplitude in fibers challenged by elevated glucose. Muscle fibers from type 1 diabetic mice exhibited increased NFAT5 expression and transverse tubule disruptions, but no differences in electrically evoked Ca^{2+} transients. Our results suggest the hypothesis that these changes in skeletal muscle could play a role in the pathophysiology of acute and severe hyperglycemic episodes commonly observed in uncontrolled diabetes.

Keywords

hyperglycemia; hypertonic stress; NFAT5; transverse tubular network; calcium; skeletal muscle

Corresponding authors: Martin F Schneider and Erick O Hernández-Ochoa. mschneid@umaryland.edu and ehern001@umaryland.edu.

Author contributions: All authors participated in the design, interpretation of the studies, analysis of the data and review of the manuscript. EOH-O performed the majority of experimentation, analysis and writing involved with this work. PR, MC and TS contributed to all aspects of this work, particularly in experimental design and interpretation of results. ZZ contributed to experimental design, discussion, critically revised the final manuscript and provided the diabetic and sham control mice. MFS contributed to experimental design, analysis, discussion and writing. All the experiments presented above were performed in the laboratory of MFS, University of Maryland, Baltimore.

Introduction

The nuclear factor of activated T-cell (NFAT) transcription factors decode signals to the nucleus from a diverse variety of extracellular messages and are required for cellular adaptation and development.[1,2] NFAT5, also known as TonEBP or OREBP, belongs to the Rel family of transcription factors, which also includes (NFATc1–4) and nuclear factor kappa B (NF-κB).[3–5] NFAT5 is not only a key regulator in protection from hypertonic stress in kidney epithelial cells from the renal medulla,[6,7] but also plays a protective role in diverse cell types ranging from macrophages and endothelial cells to cardiomyocytes and brain cells.[6,8–17] Although NFAT5 has some constitutively active transcriptional activity, its activity is modified by changes in extracellular tonicity.[3,18–20] Hypertonicity induces NFAT5 nuclear translocation and activates genes responsible for the transport and synthesis of organic osmolytes (sodium/myo-inositol transporter, SMIT), the taurine transporter, the betaine/gamma-aminobutyric acid transporter, the vasopressin-regulated urea transporter and aldose reductase (AR).[21–24] NFAT5 also induces the expression of heat-shock protein 70 and the water channel AQP2.[25,26] The NFAT5-mediated adaptive transcriptional responses to hypertonicity described above have been extensively studied in kidney-derived epithelial cells; a cell type adapted to function under large variations in osmolarity during normal physiological function *in vivo*.[18,27]

It is likely that certain pathological conditions involving alterations in osmotic balance, such as diabetic hyperglycemia or severe dehydration, also require osmotic adaptative responses in other cell types as well. NFAT5 mRNA is expressed in skeletal muscle,[4] but it is not known if skeletal muscle NFAT5 activity is modulated by osmotic stress. Glucose plasma levels during a hyperglycemic crisis in uncontrolled diabetes can reach extreme values as high as 600–1300 mg/dL (33–72 mmol/L), changing the osmolarity significantly (320–380 mOsm/kg).[28,29] In addition, there is evidence that osmotic stress elicits a morphological disruption of the transverse tubular system and abnormal Ca^{2+} signals in skeletal muscle fibers.[30–32] Therefore, it is likely that adaptive responses to and/or deleterious effects of osmotic stress play a role in the muscle pathophysiology of hyperglycemia in diabetes. Although skeletal muscle constitutes a relatively large capacity osmoregulatory pool, the possibility of osmoregulatory responses in muscle during hyperglycemia, and the corresponding underlying signaling mechanisms have, surprisingly, not been previously examined to our knowledge.

Here, we seek to evaluate the effects of elevated extracellular glucose on (1) endogenous NFAT5 activity; (2) on transverse tubule morphology; and (3) on intracellular resting Ca^{2+} levels and action potential-evoked Ca^{2+} transients using adult skeletal muscle fibers from normal and type 1 diabetic mice exposed to elevated glucose concentrations in culture. Our results provide the first account of activation of NFAT5 signaling in skeletal muscle mediated by glucose hypertonicity, and the effects of elevated glucose on tubular system morphology and electrically evoked Ca^{2+} signals in skeletal muscle.

Materials and methods

Flexor digitorum brevis skeletal muscle fibers culture

Experiments were performed on skeletal muscle fibers enzymatically isolated from the *flexor digitorum brevis* (FDB) muscles of four- to five-week-old C57BL/6J mice. Animals were euthanized by CO_2 exposure followed by cervical dislocation before removal of the muscles according to protocols approved by the University of Maryland Institutional Animal Care and Use Committee. FDB skeletal muscle fibers were isolated, dissociated and cultured in a humidified incubator at 37°C (5% CO_2) as previously described.[33–36] Fibers were cultured on laminin-coated glass-bottom culture dishes. After plating, cultures were

maintained in minimum essential media (Invitrogen, Eugene, OR, USA; containing 5.56 mmol/L D-glucose, supplemented with 10% fetal bovine serum and 50 μg mL^{-1} gentamicin sulfate). This media formulation was used as control/isotonic media (288 mOsm/kg). During the first day after plating, fibers were treated with cytosine β-D-arabinofuranoside (ara-C) 10 μmol/L for 24 h to reduce proliferating non-muscular cells and to delay the fiber de-differentiation process[33,36] (see protocol on Figure 1b). For fibers challenged with elevated extracellular glucose media, either D- or L-glucose (25 or 50 mmol/L) was added to the control isotonic media. Over an isotonic baseline of 288 mOsm/kg, addition of 25 mmol/L D-glucose raised the osmolality to 308 mOsm/kg, and 50 mmol/L D-glucose to 336 mOsm/kg. Osmolarity of the culture medium was measured in a Vapro-5520 Osmometer (Wescor, Inc., Logan, UT, USA). Where indicated, the fibers were five-day cultured when used. In the experiments using diabetic mice, fibers were not treated with ara-C and were used within the first day after isolation.

Chemically induced type 1 diabetic animal model

The procedure for generation of type 1 diabetic mice was conducted as previously described[37] and following procedures approved by the University of Maryland Institutional Animal Care and Use Committee. Briefly, female C57BL/6J mice (median body weight 22 g) were purchased from Jackson Laboratory (Bar Harbor, Maine, ME, USA). Streptozotocin (STZ) from Sigma (St Louis, MO, USA) was dissolved in sterile 0.1 mol/L citrate buffer (pH 4.5). Eight-week-old C57BL/6J mice were intravenously injected daily with 65 mg/kg STZ for three days to induce diabetes. Insulin pellets were subcutaneously implanted in diabetic mice to restore euglycemia to mimic insulin treatment. After five days, insulin pellets were removed to permit frank hyperglycemia. When blood glucose levels reached ≤250 mg/dL, the animals were considered diabetic. Plasma glucose levels were measured from tail vein samples using a commercially available kit (One Touch UltraMini; LifeScan, Milpitas, CA, USA) according to the manufacturer's instructions. Mice were euthanized after experiencing 10 days of continuous hyperglycemia. Animals injected with the citrate buffer served as euglycemic controls. Tibialis anterior (TA) muscles were dissected and used for Western blot assays. Individual fibers from FDB muscles were isolated and plated as described above and used within the first 24 h.

Dual-luminescence-based gene reporter assays

Approximately 100–150 FDB fibers/dish were transferred to serum-free, isotonic control medium 48 h after plating and ara-C treatment. After serum removal, fibers were co-transfected with adenovirus encoding a luciferase-based reporter of NFAT activity (9X-NFAT-luciferase[38]) and a second adenovirus encoding constitutively active β-galactosidase under the control of a cytomegalovirus (CMV) promoter at a ratio of 5:1. The fibers were exposed to hypertonic (308–336 mOsm/kg) high-glucose media (D- or L-glucose; 25–50 mmol/L) 24 h after transfection and returned to a culture incubator for an additional 6–48 h. Fibers from each dish were lysed and the activity of each reporter measured on a manual luminometer (Tropix) using the Dual-Light System (Applied Biosystems, Bedford, MA, USA). The expression of firefly luciferase was normalized to the constitutively expressed β-galactosidase activity to correct for differences in transfection efficiency. Each experiment was conducted in duplicate or triplicate and repeated at least three times on cultures prepared from separate litters.

Protein extraction and Western blots

Culture plates containing fibers from FDB muscles or TA whole muscle homogenates provided a sufficient amount of cellular material for Western blot experiments. These procedures have been described previously.[39] An independent experiment consisted of cultured isolated fibers from two whole FDB muscles, or one whole TA muscle, 3–4 mice

per group. Briefly, FDB fibers were transferred to phosphate-buffered saline (PBS) 48 h after plating and ara-C treatments. Cultured FDB fibers or TA muscles were homogenized with a mammalian protein extraction reagent (M-PER; Pierce, Rockford, IL, USA) supplemented with protease inhibitor cocktail (Complete-Mini EDTA-free; Roche Diagnostics, Indianapolis, IN, USA). The homogenates were subjected to centrifugation at 10,000 rpm for 10 min at 4°C. The supernatant was extracted and stored. Protein concentrations were measured using a Nanodrop-1000 spectrophotometer (Thermo Scientific, Wilmington, DE, USA). Samples for electrophoresis were not boiled, but were solubilized at 70°C for 10 min. Then, 40 μg protein samples were fractionated by 4–12% sodium dodecyl sulfate-polyacrylamide gel electrophoresis and transferred to nitrocellulose membrane, at 20 V for three hours at 4°C using the Xcell II blot module (Invitrogen). Blots were then processed and probed with antibodies against NFAT5 (1:1000; Cat No. sc-101098; Santa Cruz Biotechnology, Inc., Santa Cruz, CA, USA), SMIT (1:1000; Cat. No. H00006526-M02; Abnova, Taipei, Taiwan), AR (1:1000; Cat. No. H00000231-B01P; Abnova) and glyceraldehyde-3-phosphate dehydrogenase (GAPDH; 1:12000; Cat. No. G8795; Sigma). Blots were incubated with the appropriate horseradish peroxidase (HRP)-labeled secondary antibodies (KPL, Gaithersburg, MD, USA). Films were developed following exposure to sensitive enhanced chemiluminescent substrate to detect HRP on immunoblots. Either SuperSignal West Pico or the more sensitive SuperSignal West Femto were used (Pierce). ImageJ (NIH, Bethesda, MD, USA; http://rsb.info.nih.gov/ij/) was used to analyze data. The relative levels of each protein were calculated as a ratio against GAPDH and then normalized to those of controls run in the same gel.

Immunocytofluorescence

Fibers were fixed in PBS (pH 7.4) containing 4% (w/v) of paraformaldehyde for 15 min and then permeabilized in PBS containing 0.1% (v/v) Triton ×100 (Sigma) for 15 min. The fibers were exposed to PBS containing 8% (v/v) of donkey serum for one hour at 4°C to block non-specific labeling. The fibers were first incubated with a primary antibody against the C-terminal residues 1439–1455 of NFAT5 (1:400, overnight at 4°C; Cat No. ab3446; Abcam, Cambridge, MA, USA), followed by incubation with Alexa-488-conjugated donkey anti-mouse antibody (1:200 dilution, 2 h at room temperature; Invitrogen). Dishes were washed thoroughly after each step in PBS containing 2% (v/v) of donkey serum. For each primary antibody-treated dish, another dish was treated with the secondary antibody only and used as control. 4',6-Diamidino-2-phenylindole (DAPI; 10 μmol/L; for 30 min; Invitrogen) was used to stain the nuclei. Antibody-labeled and DAPI stained fibers were imaged on a Zeiss LSM 5 Live system, based on an Axiovert 200M inverted microscope (Carl Zeiss Microimaging, Inc., Thornwood, NY, USA) using a 63× NA 1.2 water immersion objective lens. The excitation for Alexa-488 and DAPI were provided by using 488 and 405 nm lasers, respectively. The emitted light for Alexa-488 was collected at > 510 nm. DAPI emission was collected between 420 and 480 nm. Confocal images of randomly selected fibers exposed to either isotonic or high-glucose/hypertonic conditions were collected and evaluated blindly, using the same image acquisition settings and enhancing parameters so that all images could be directly compared. Images were background corrected, after which cytoplasmic and nuclear regions of fixed dimensions were used to estimate average fluorescence within the regions of interest. These values were then used to calculate nuclear/cytosolic ratios and were expressed as arbitrary units (A.U.). Images were processed using custom-written software in IDL (RSI, Boulder, CO, USA) and ImageJ (NIH; http://rsb.info.nih.gov/ij/).

Time-lapse imaging

Long-term live cell incubation and an imaging system (Vivaview FL Incubator; Olympus, Center Valley, PA, USA) were used, where indicated. Fibers were maintained in control

media (5.56 mmol/L D-glucose) MEM containing 1% fetal bovine serum and 50 μg mL^{-1} gentamicin sulfate in 5% CO_2 (37°C). Where indicated, fibers were challenged with hypertonic/high-glucose media (25 or 50 mmol/L D-glucose). Time-lapse imaging was conducted for up to 96 h at 10-min acquisition intervals using a 20× objective magnification.

Indo-1 ratiometric recordings

Indo-1 acetoxymethyl (AM) ratiometric recording and analysis were performed as previously described[40] but with some modifications for loading. Briefly, cultured FDB fibers were loaded with indo-1AM (2 μmol/L for 30 min at 22°C; Invitrogen) in L-15 media (ionic composition in mM: 137 NaCl, 5.7 KCl, 1.26 $CaCl_2$, 1.8 $MgCl_2$, pH 7.4; Invitrogen) with or without 25–50 mmol/L of added D- or L-glucose. Then the fibers were washed thoroughly with appropriate L-15 media to remove residual Indo-1AM and incubated at 22°C for another 30 min to allow dye conversion. The culture dish was mounted on an Olympus IX71 inverted microscope and viewed with an Olympus 60×/1.20 NA water immersion objective. Fibers were illuminated at 360 nm, and the fluorescence emitted at 405/30 and 485/25 nm was detected simultaneously. The emission signals were digitized and sampled at 10 Hz using a built-in AD/DA converter of an EPC10 amplifier and the acquisition software Patchmaster (HEKA Instruments Inc., Bellmore, NY, USA). Field stimulation (1 ms, 8 V, alternating polarity) was provided by a custom pulse generator through a pair of platinum electrodes. The electrodes were closely spaced (0.5 mm) and positioned directly above the center of the objective lens, to achieve semi-local stimulation. Fluorescence ratios (R = F405/F485) were converted to free myoplasmic Ca^{2+} concentration ($[Ca^{2+}]_i$) according to the equation: $[Ca]_i = Kd^* \beta^* [(R–R_{min})/(R_{max}–R)]$[41] using an *in vivo* Kd of 394 nmol/L.[42] R_{min} and R_{max} are limiting values for R at zero and saturating $[Ca^{2+}]$, respectively. R_{min} and R_{max} were estimated as previously described.[33]

Transverse tubular network imaging in living fibers

Control or high-glucose-exposed FDB fibers were stained with the voltage-sensitive dye pyridinium, 4-[2-(6-(dioctylamino)-2-naphthalenyl) ethenyl]-1-(3-sulfopropyl)-, inner salt (di-8-ANEPPS) (5 μmol/L; in L-15 media for 1 h) and imaged on a Fluoview 500 confocal system (Olympus; ×60, 1.3 NA water-immersion objective; pixel dimensions 0.2 × 0.2 μm in x and y). Confocal images of the tubular network were obtained with 512 × 512 pixel x–y images (average of eight images). Images from fibers exposed to either control or high-glucose conditions were collected from randomly selected fibers using the same image acquisition settings and enhancing parameters. Images were background corrected and a region of interest of fixed dimensions was used to estimate average fluorescence profile within the region of interest.

Data analysis and statistics methods

Electrophysiology and indo-1 data were analyzed and plotted using Patchmaster, Fitmaster (HEKA Instruments Inc.). Immunocytochemistry, di-8-ANEPPS signals and Western blot data were analyzed with ImageJ. Further data evaluation and statistical analysis were conducted using OriginPro 8 software (OriginLab Corporation, Northampton, MA, USA). Summary data were reported as mean ± SEM when samples followed normal distributions and as medians when samples were less well defined. Box plots and bar graphs were used for graphic illustration of data. Statistical significance was assessed using either parametric two sample t-test or with the non-parametric Mann–Whitney rank-sum test for unpaired data sets.

Results

Elevated glucose activates NFAT-mediated gene transcription and NFAT5 protein expression in cultured FDB fibers

We first evaluated if skeletal muscle NFAT5 signaling is activated by elevated extracellular glucose. Blood glucose levels are closely regulated in healthy individuals and rarely stray outside the range 4.2–6.4 mmol/L, but can reach high values between 7 and 25 mmol/L in individuals with diabetes mellitus and in animal models of diabetes.[43–47] Hyperglycemia is commonly found to be even more extreme (30–70 mmol/L) in patients with uncontrolled diabetes. During such extreme events, life-threatening acute metabolic complications of diabetes such as hyperglycemic hyperosmolar state (HHS) can occur.[28,29] These episodes of severe hyperglycemia (i.e. ≥30 mmol/L glucose) might be accompanied by a substantial increase in plasma tonicity. It is likely that hyperglycemia and associated hypertonicity initiate adaptive responses to osmotic stress.

To address this possibility, we sought to experimentally reproduce this condition. Skeletal muscle fibers isolated from control mice were exposed to media conditions mimicking sustained and extreme elevated glucose. We used an adenoviral system carrying a firefly luciferase reporter driven by nine copies of NFAT binding sites[38] together with a control adenovirus encoding a reporter of β-galactosidase driven by the constitutively active CMV promoter to evaluate if elevated glucose resulted in the activation of NFAT-dependent transcriptional activity (Figure 1a). The time course of the experimental protocol used in these studies is illustrated in Figure 1b. We found that the NFAT-luciferase reporter was activated after 24 h of exposure to glucose levels of 25 and 50 mmol/L when compared with control counterparts (5.56 mmol/L D-glucose; Figure 1c). Fibers exposed for 24 h to high glucose (50 mmol/L added D- or L-glucose) also exhibited elevated NFAT5 protein expression (Figures 1d and e). The effects mediated by D-glucose at the level of NFAT-dependent transcriptional activity as well as those on NFAT5 protein expression were comparable to those observed in fibers challenged with the same concentration of non-transportable, metabolically inert L-glucose (Figures 1c and e), suggesting an osmoadaptive rather than metabolic effect. These results indicate that osmotic stress in adult skeletal muscle fibers due to elevated extracellular glucose induces NFAT-dependent transcriptional activity as well as increases NFAT5 protein expression levels.

NFAT-dependent transcriptional activity induced by elevated extracellular glucose does not involve Ca^{2+}/calcineurin-dependent NFATc isoforms

It has been shown that 9X-NFAT-luciferase reporter can be used to detect the activities of both the Ca^{2+}-sensitive NFAT isoforms (NFATc1–4) and the Ca^{2+}-independent NFAT5 in primary cells.[11,38] In order to address if NFAT-luciferase reporter was activated by NFATc1–4 or by NFAT5, in our experiments, we used FK506 to inhibit calcineurin A (CnA) activity, and hence the activation of all the Ca^{2+}/CnA-dependent NFAT isoforms (NFATc1–4). For these experiments, fibers were pretreated with FK506 at 250 nmol/L for two hours prior to as well as during the challenge with high glucose (50 mmol/L; 48 h), and compared with fibers without FK506. Figure 2a shows that NFAT-luciferase reporter activity of fibers exposed to high glucose was not suppressed by the CnA inhibitor FK506. We also monitored NFAT5 protein expression in cells pretreated with the FK506 and then challenged with high glucose and found that the inhibition of CnA does not reduce the increment in NFAT5 protein expression observed in fibers challenged with high glucose (Figure 2b). Our results instead show a moderate increase of both NFAT-luciferase and NFAT5 protein expression in fibers pretreated with FK506 and challenged with high glucose. These results indicate that Ca^{2+}/calcineurin-dependent NFATc isoforms are not

involved in the elevated NFAT-luciferase reporter activity and augmented NFAT5 expression seen in fibers exposed to high glucose.

Inhibition of stress kinases p38α and PIKK reduces transcriptional activation of NFAT and NFAT5 protein expression in response to high glucose challenge

Activation of NFAT5 by osmotic stress is complex and may be regulated by a variety of different intracellular signaling pathways whose relative contributions vary among different cell types.[18] Depending on the cell type, the activation of NFAT5 may be regulated by signaling pathways that involve stress-activated kinases such as p38 mitogen-activated protein kinases (MAPK), phosphoinositide 3-kinase and DNA-damage-activated phosphoinositide 3-kinase-related kinase (PIKK), Fyn, a shrinkage-activated tyrosine kinase (PKA) and extracellular-signal-regulated kinases,[48–53] as well as other enzymes such as phospholipase C_γ and Src homology phosphatase-1, a protein phosphatase.[54,55] However, the combination of PIKK and p38α MAPK seems to be essential in primary cell cultures.[18,49,56] Therefore, to investigate the contribution of these kinases on the NFAT-luciferase reporter activity and NFAT5 protein expression induced by high glucose in skeletal muscle fibers, we used inhibitors of p38α MAPK (SB203580) and PIKK (LY294002). As shown in Figure 3a, the NFAT-luciferase reporter activity of fibers exposed to high glucose was sensitive to pretreatment with p38α MAPK inhibitor (SB203580; 10 μmol/L) and the PIKK inhibitor (LY294002; 25 μmol/L). The combined action of both inhibitors produced a slightly larger but still incomplete reduction of the NFAT-luciferase reporter activity (Figure 3a). Figure 3b shows that the inhibition of both p38α and PIKK produced almost a complete suppression of the increase in NFAT5 expression seen in the untreated high-glucose-exposed counterpart. These results implicate p38α MAPK and PIKK (SB203580- and LY294002-sensitive kinases, respectively) in both the transcriptional activation of NFAT5 and in the regulation of its expression in response to high glucose-dependent osmotic stress.

Distribution of endogenous NFAT5 and increased nuclear translocation in fibers exposed to high extracellular glucose

Next, we sought to determine the subcellular distribution of endogenous NFAT5 in skeletal muscle fibers and its potential translocation in fibers challenged with elevated extracellular glucose. To this end, we utilized confocal microscopy to image endogenous NFAT5 in fixed fibers stained with a monoclonal antibody against NFAT5 using indirect immunofluorescence. Figure 4 shows representative confocal images of the NFAT5 intracellular distribution and DAPI staining, to identify the nuclear location and intranuclear structure, in both control (5.56 mmol/L D-glucose, Figure 4a) and high-glucose-exposed fibers (50 mmol/L added D-glucose, Figure 4b). In control fibers, NFAT5 was present in both the cytosolic and nuclear compartments, indicating a constitutive nuclear presence of NFAT5 in resting cells (Figure 4a, top panel), as previously observed in other cell types.[3,4,18,20,27] NFAT5 was also present in both the cytosolic and nuclear compartments in fibers exposed to elevated glucose (Figure 4b, top panel). However, the nuclear/cytosolic ratio, a metric of nuclear translocation, was significantly larger in high-glucose-exposed fibers than in the control counterparts (2.39 ± 0.18 for high-glucose-exposed fibers versus 1.81 ± 0.08 for control fibers; $P < 0.05$, $n = 14$ fibers per group, Figure 4c). These results indicate greater nuclear translocation in fibers challenged with high glucose. As illustrated in Figures 4a and b, the intranuclear distribution of NFAT5 is not homogenous; instead, it showed a distinct pattern of fluorescent foci (Figures 4a and b, asterisks). The number of foci in each nucleus varied between different nuclei in the same or different fibers (1–3 foci per nucleus of about 1–3 μm in diameter). Such foci were observed in all nuclei of control and high-glucose-exposed fibers.

Elevated glucose increased protein expression of aldose reductase and sodium/myo-inositol transporter

Long-term exposure to hypertonic conditions results in altered transcription of a number of osmoregulatory genes, most of which are involved in uptake and synthesis of non-ionic osmolytes (such as sorbitol, inositol, betaine, amino acids and their derivatives), heat-shock proteins and aquaporins.[21–26] In order to evaluate if a sustained elevation in glucose results in the activation of osmoprotective genes in skeletal muscle, we examined the protein expression levels for AR, which catalyzes the reduction of glucose to sorbitol, and of the sodium/myo-inositol transporter SMIT, which is involved in the uptake of inositol. About 75% increase in AR expression was detected 24 h after an elevation in extracellular D-glucose (50 mmol/L; Figures 5a and b, $P < 0.05$) when compared with the control (5.56 mmol/L) counterpart. A more modest but significant increase in SMIT was also seen in fibers challenged with high glucose (Figure 5, $P < 0.05$). These results indicate that in skeletal muscle fibers, a sustained elevation in extracellular D-glucose increases the expression of osmoregulators, most notably AR.

Fibers exposed to elevated glucose do not exhibit major changes in gross morphology

The preceding section demonstrating NFAT-transcriptional activation, NFAT5 protein expression and the increased expression of AR induced by elevated glucose indicates that FDB muscle fibers are endowed with osmoprotective responses. Next, we evaluated the effects of elevated glucose on single muscle fiber gross morphology. Figure 6 shows representative differential interference contrast microscopy images from a 72-hour time-lapse experiment using a microscope-incubator (see Materials and methods). Cultured FDB fibers were maintained at 37°C before and during a control medium change (isotonic control to isotonic control, 5.56 mmol/L D-glucose; Figure 6a), exposure to 25 mmol/L added D-glucose (Figure 6b) or during exposure to 50 mmol/L added D-glucose (Figure 6c). In general, the vast majority of the fibers were able to with-stand the challenge with 25–50 mmol/L D-glucose for up to 48 h without displaying any major change in morphology, such as a dramatic reduction in the fiber's width or length, and with a well-maintained sarcomeric pattern. These observations indicate maintenance of the longitudinal pattern of repeated thick and thin filament arrays.[57] However, 5% of fibers exposed to 50 mmol/L D-glucose developed irreversible contracture followed by fiber lysis, which was not seen in fibers in isotonic solution.

High-glucose-exposed fibers exhibit a highly disrupted transverse tubular network

The transverse tubular system architecture is essential for muscle contraction.[58–60]

Since sustained hyperosmotic stress might be related to changes in transverse tubular morphology, we next sought to evaluate transverse tubular organization in cultured fibers under both control and high-glucose conditions using the lipophilic dye di-8-ANEPPS, which stains both the surface sarcolemma and the tubular system due to their exposure to the extracellular solution. In adult mammalian skeletal muscle, the transverse tubular system displays a highly organized transverse pattern, with a transverse tubular system located at each of the two A/I boundaries in each sarcomere. Figure 7a shows that overall transverse tubular morphology is preserved in five-day cultured fibers maintained in isotonic control (5.56 mmol/L D-glucose) media. Transverse tubules in the control fibers were organized in a regular striated pattern, characterized by a ~2 μm sarcomere length and ~1 μm tubule `doublet' spacing. This pattern is similar to one observed in one-day-old cultured fibers,[33] suggesting that five-day cultured control fibers maintain a normal intact transverse tubular system after exposure to ara-C. In fibers exposed to ara-C and cultured for five days, in 25 mmol/L (Figure 7b) or 50 mmol/L (Figure 7c) glucose, the transverse tubular system appeared disorganized, characterized by a disruption of the regular transverse striated

pattern across the fiber. A common observation in fibers exposed to 50 mmol/L D-glucose for 48 h was the presence of segmental tubular swelling (Figure 7c, stars) and in some regions a more pronounced reorganization was characterized by zones of proximity between adjacent transverse tubules (Figure 7c, arrows), a feature typical of longitudinal tubules. These results indicate that in fibers exposed to sustained elevated extracellular glucose, the transverse tubular system architecture is disrupted and appears to be undergoing reorganization.

Fibers from diabetic mice exhibit elevated levels of NFAT5 protein expression and disrupted transverse tubular system morphology, but normal Ca^{2+} homeostasis

The experiments described above examined the effects of elevated extracellular glucose on NFAT transcriptional activity, NFAT5 expression and transverse tubule morphology in cultured FDB fibers isolated from healthy control mice artificially exposed to elevated glucose. Seeking to better understand the pathophysiological effects of sustained glucose elevation in uncontrolled diabetes, we next investigated if NFAT5 expression levels were altered in muscle fibers isolated from a chemically induced mouse model of type 1 diabetes exhibiting hyperglycemia (see Materials and methods). As a control, we used muscle fibers isolated from aged-match sham, citrate-injected, non-diabetic mice. Plasma glucose concentrations immediately after euthanasia procedure were 8.1 ± 0.2 mmol/L ($n = 4$) in control mice and 22.8 ± 5.0 mmol/L ($n = 4$) in diabetic mice. Average and peak plasma glucose concentrations sampled from living diabetic mice were 20 ± 6 and 28 ± 3 mmol/L, respectively. These measurements are consistent with previous studies indicating that plasma glucose levels range between 6 and 10 mmol/L in non-diabetic animals and about 20–25 mmol/L in animal models of diabetes.[43–46] Fibers from diabetic mice exhibited elevated NFAT5 protein expression when compared with the sham counterpart (Figure 8a).

Next, we asked if fibers from diabetic mice exhibit changes in transverse tubular morphology. Figure 8c shows that in one-day-old cultured fibers from diabetic mice, the transverse tubular system was disorganized, and characterized by a disruption of the regular pattern running transversely across the fiber. A larger number of zones of proximity between adjacent transverse tubules were also identified (Figure 8c, arrows). These observations partially recapitulate what we observed in fibers from non-diabetic mice exposed to elevated (25 mmol/L) glucose. In clear contrast, transverse tubule morphology was unaltered in one-day-cultured control fibers from sham, non-diabetic mice (Figure 8b).

Because of the T-system disruption, we also investigated the effects of hyperglycemia on Ca^{2+} homeostasis and action potential evoked Ca^{2+} transients in muscle fibers dissociated from diabetic mice and sham non-diabetic mice. Figure 8d illustrates the average time course of indo-1 signals before and after field stimulation for 31 fibers from sham, non-diabetic mice (black trace) and 35 fibers from diabetic mice. Fibers from diabetic mice having a serum glucose value of 22 mmol/L did not exhibit significant changes in resting indo-1 ratio (resting $[Ca^{2+}]_i$ was 31 nmol/L in diabetic fibers versus 37 nmol/L in control, non-diabetic fibers, $P > 0.05$; Figure 8e). A non-statistically significant difference in average peak $[Ca^{2+}]_i$ was observed in fibers from diabetic mice (peak $[Ca^{2+}]_i$ was 438 nmol/L in diabetic fibers versus 456 nmol/L in control, non-diabetic fibers, $P > 0.05$; Figures 8d and e). The above results indicate that fibers from diabetic mice exhibit increased NFAT5 expression and alterations in transverse tubular architecture but no changes in Ca^{2+} homeostasis and electrically evoked Ca^{2+} transients.

Fibers from control mice experimentally exposed to elevated glucose exhibit increased action potential-induced Ca^{2+} signals

In order to explore the effects of extremely elevated glucose on resting intracellular Ca^{2+} concentration ($[Ca^{2+}]_i$) and electrically evoked Ca^{2+} transients, fibers from control mice were experimentally challenged with 25 or 50 mmol/L D- or L-glucose. We subjected fibers to sustained glucose exposure (48 h, see protocol Figure 9a), and monitored indo-1 ratio signals at rest and the amplitude of electrically evoked indo-1 Ca^{2+} transients in the continued presence of elevated glucose. Figure 9b illustrates the average time course of indo-1 signals elicited by brief electric field stimulation at time zero (1 ms, 8–12 V) for 31 fibers in control (black trace), 18 fibers exposed to 25 mmol/L D-glucose (cyan trace) and 11 fibers exposed to 25 mmol/L L-glucose (red trace). We did not observe significant differences in resting $[Ca^{2+}]_i$ or in the amplitude of AP-evoked Ca^{2+} transients in fibers exposed to 25 mmol/L D-or L-glucose (Figures 9b–d) when compared with the control counterpart. The resting $[Ca^{2+}]_i$ was 59 nmol/L in 25 mmol/L D-glucose-exposed fibers, 53 nmol/L in 25mmol/L L-glucose-exposed fibers, versus 50 nmol/L in control fibers, $P > 0.05$; the peak $[Ca^{2+}]_i$ was 329 nmol/L in 25 mmol/L D-glucose-exposed fibers, 269 nmol/L in 25 mmol/L L-glucose-exposed fibers versus 270 nmol/Lincontrol fibers, $P > 0.05$.

Figure 9c illustrates the average time course of indo-1 signals elicited by the same brief electric field stimulus for 24 fibers in control (black trace), 21 fibers exposed to 50 mmol/L D-glucose (cyan trace) and 20 fibers exposed to 50 mmol/L L-glucose (red trace). We did not observe a significant change in resting $[Ca^{2+}]_i$ in fibers exposed to 50 mmol/L elevated D-glucose (Figure 9e) when compared with the control counterpart (resting $[Ca^{2+}]_i$ was 61 nmol/L in high D-glucose-exposed fibers versus 65 nmol/L in control fibers, $P > 0.05$). A statistically significant reduction in resting $[Ca^{2+}]_i$ was observed in fibers challenged with L-glucose (35 nmol/L in high L-glucose-exposed fibers versus 65 nmol/L in control fibers, $P < 0.05$; Figure 9e).

Fibers exposed to 50 mmol/L D-glucose exhibited a larger electrically evoked Ca^{2+} transient on average (Figures 9c and e; estimated peak $[Ca^{2+}]_i$ was 468 nmol/L in D-glucose-exposed fibers versus 358 nmol/L control fibers, $P < 0.05$). A non-statistically significant difference in average peak indo-1 ratio and estimated $[Ca^{2+}]_i$ was observed in fibers challenged with L-glucose (Figure 9e; peak $[Ca^{2+}]_i$ was 326 nmol/Lin L-glucose-exposed fibers versus 358 nmol/L in control fibers, $P > 0.05$). The effects of 50 mmol/L D-glucose on electrically evoked Ca^{2+} transients were not comparable to those observed in fibers challenged with the same concentration of metabolically inert L-glucose (Figure 9e), suggesting the possibility of a metabolic rather than an osmoadaptive effect. The above results indicate that sustained 50 mmol/L elevated D-glucose does increase the amplitude of average AP-induced Ca^{2+} transients with no effect on resting calcium levels.

Discussion

Relatively little is known about the behavior of NFAT5 in adult muscle fibers in response to hypertonicity. In particular, the effect of elevated extracellular glucose on single adult fibers has not, to our knowledge, previously been investigated. Our results show that NFAT5 is endogenously expressed in adult murine skeletal muscle fibers, and that elevated extracellular glucose enhances NFAT-dependent transcriptional activity, NFAT5 nuclear translocation and NFAT5 expression levels. Endogenous NFAT5 is present in both cytoplasmic and nuclear compartments in control adult murine skeletal muscle fibers, indicating a small constitutive nuclear presence of NFAT5 in resting cells, as previously reported in other cell types.[3,4,18,20,27] Elevation of extracellular glucose causes a significant increase in NFAT5 nuclear translocation. In both control and high-glucose-exposed fibers, NFAT5 exhibits non-uniform nuclear distribution with intranuclear foci (1–3 foci per

nucleus of about 1–3 μm in diameter) of elevated concentration. Our laboratory have previously demonstrated that Ca^{2+}/calcineurin-dependent dephosphorylation of NFATc1 during repetitive skeletal muscle activity causes NFATc1-green fluorescent protein (GFP) nuclear translocation and concentration in subnuclear NFAT foci.[35] Recent data from our laboratory demonstrated that NFATc1-GFP nuclear foci co-localize with heterochromatin regions of intense staining by DAPI that are present in the nucleus prior to NFATc1 nuclear entry and that mutation of the NFATc1 DNA-binding sites prevents entry and localization of NFATc1 in heterochromatin regions, and fluorescence *in situ* hybridization showed that the NFAT-regulated genes for slow and fast myosin heavy chains are not localized within the heterochromatin regions, indicating that NFATc1 foci may serve as nuclear storage sites for NFATc1.[61] Here, we showed that endogenous NFAT5 nuclear foci do not co-localize with heterochromatin regions of intense staining by DAPI. Further studies are required to test if NFAT5 within the nuclear foci is directly related to activation of its target genes and to analyze the molecular basis underlying the formation of nuclear NFAT5 foci.

NFAT-transcriptional activity was sensitive to pharmacological kinase inhibitors involved in the activation of NFAT5 but was insensitive to the calcineurin A inhibitor, FK506. This indicates a selective activation of the NFAT-luciferase reporter, likely via NFAT5, in response to osmotic stress without the involvement of Ca^{2+}/calcineurin-dependent NFATc1–4 isoforms. NFATc1–4 and NFAT5 differ substantially in their mechanisms of activation and biological function. NFAT5 is activated by osmotic stress,[4,18,20] whereas NFATc isoforms are characteristically activated by the phosphatase calcineurin in response to increases in intracellular calcium concentration.[1,2,35] Our findings support the idea that the specific recruitment of either NFAT5 or NFATc iso-forms to DNA binding sites is stimulus-dependent.[11] High glucose-dependent activation of NFAT-luciferase reporter was considerably reduced by LY294002, a PIKK inhibitor and by SB203580, a p38 MAPK inhibitor. These results are in agreement with a previous report using T cells and HEK293 cells.[53] We also found that inhibition of PIKK and p38 reduced the upregulation of NFAT5 expression by high-glucose-dependent osmotic stress. It has been reported that both a dominant negative p38 construct and SB203580 effectively inhibited a luciferase reporter gene under the control of osmotic response element in embryonic fibro-blasts.[50] Chen *et al.*[62] found that NFAT5 associated with tonicity-responsive enhancer in a tonicity-dependent fashion in cultured rat renal medullary cells, and blockade of NFAT5 activity with the p38 inhibitor (SB203580) resulted in suppression of the osmotic induction of the Sgk1 promoter. However, it is important to interpret our results using kinase inhibitors with caution. We cannot conclude that all the observed effects on NFAT-luciferase reporter activity and upregulation of NFAT5 arise exclusively from the regulation of p38 and PIKK kinases. Although SB203580 and LY294002 are very useful, recent studies have indicated that they inhibit other protein kinases with similar or even greater potency.[63] Nevertheless, our characterization of the sensitivity of NFAT-luciferase reporter and NFAT5 protein expression to pharmacological kinase inhibitors in skeletal muscle fibers, together with previous reports, supports the idea that activation of NFAT5 by osmotic stress involves several signaling pathways, with PIKK and p38 as common regulators.[18,50,53,56] Unraveling the exact identity of signaling molecules (kinases and phosphatases), mechanisms and targets of NFAT5-regulatory pathways in skeletal muscle is the subject of ongoing investigations.

Contrary to what is typically found in cells from the renal medulla which are exposed physiologically to a hypertonic environment with osmolality values around 1000 mOsm/kg,[6,20,27] our experiments show that NFAT-dependent transcription and NFAT5 expression in skeletal muscle fibers are sensitive to moderate increases in extracellular osmolality (315–330 mOsm/kg). Importantly, serum osmolality levels >320 mOsm/kg are a common clinical finding in the plasma of patients with acute complications of diabetes.[28,29,64–66] Our

findings and previous observations reported in primary cells such as lymphocytes, macrophages, fibroblasts[11] and cardiomyocytes,[17] indicate a lower threshold for NFAT5 activation in cells that are not physiologically exposed to a hypertonic environment. Altogether, these observations and our results indicate that extreme and abnormally sustained elevations of the extracellular glucose activate an osmoprotective and adaptative response in skeletal muscle via the expression and transcriptional activation of NFAT5.

In skeletal muscle fibers, acute osmotic stress affects the transverse tubular system.[30,32,67–70] The transverse tubular system is a continuation of the surface membrane, which invaginates into the muscle fiber at each sarcomeric A–I junction in mammalian muscle, and forms the main interface between the myoplasm and the extracellular environment.[71] The transverse tubules form junctions with the internal Ca^{2+} storage organelle of the fiber, the sarcoplasmic reticulum (SR).[58,59] These arrangements are essential for the action potential radial propagation, transverse tubular voltage sensor activation, subsequent SR Ca^{2+} release and muscle contraction in the process known as excitation-contraction (E–C) coupling.[60,72] Longitudinal tubules also form part of the tubular membrane system; they form junctions between adjacent transverse tubules and represent a small fraction of the total membrane area of the tubular system in vertebrates.[58,71,73,74] The role of the longitudinal tubules is to ensure that the transverse tubular system is an internally connected network within the muscle fiber.[74,75] Thus, the tubular system architecture is essential in the normal function of E–C coupling. Our results show dramatic disruption and reorganization of the tubular system after a two-day exposure to 50 mmol/L glucose. These changes are characterized by a substantial dilation of the peripheral transverse tubular system. Our results also show an increased number of junctions between adjacent transverse tubules in fibers challenged with elevated glucose for two days in culture or in fibers from diabetic mice, suggesting an increment of longitudinal tubules. These longitudinal tubular pathways within the fiber could be used as a compensatory or adaptive mechanism in the regions with substantial swelling of the transverse tubules. The transverse system changes seen here in fibers treated with ara-C and exposed to elevated glucose for two days and from untreated type 1 diabetic mice are reminiscent of the transverse tubular system disorganization seen in dedifferentiating fibers cultured for longer times without exposure to ara-C.[33,36]

Long-term diabetes affects skeletal muscle function in many ways, commonly including neuropathy and atrophy. Depolarization of resting membrane potential, changes in the action potential properties and reduced force and contractility are commonly found in several muscle types assayed in animal models of type 1 and type 2 diabetes.[43,44,46] It has been shown that enzymatically dissociated muscle fibers exhibit abnormal local Ca^{2+} signals under relatively brief periods of osmotic stress (ranging from seconds up to 30 min treatments) induced with hyper-tonic solutions using elevated divalent cations,[30–32] and abnormal global Ca^{2+} signals have been observed in hyper-tonic solutions using sucrose or mannitol.[31] In this study, we did not find significant changes in resting Ca^{2+} levels and electrically evoked Ca^{2+} signals in fibers isolated from diabetic mice (serum glucose: 20–25 mmol/L). However, our results clearly show alterations in Ca^{2+} signals from five-day-old cultured fibers challenged with sustained (24–48 h) elevated extracellular glucose (50 mmol/L). This scenario of sustained elevated glucose concentration is likely to occur during hyperglycemic crisis in patients with uncontrolled diabetes,[28,29] particularly during HHS, a life-threatening acute metabolic complication of uncontrolled type 2 diabetes mellitus. The classical clinical picture of HHS includes history of polyuria, polydipsia, weight loss, vomiting, dehydration, weakness and mental status changes. During episodes of HHS, which is a common condition in elderly patients and is being diagnosed with increasing frequency in obese children, plasma glucose reach levels as high as 600–1300 mg/dL (33–72 mmol/L) and an increase in serum osmolality (320–380 mOsm/kg) is typically observed. HHS usually

develops over days to weeks and the duration of these symptoms is generally for several days, with a prognosis of 10–20% mortality.[28,29]

It is important to consider that the abnormalities observed in the present report in fibers exposed to elevated glucose may be influenced by the effects of fiber denervation as may occur in our isolated cultured muscle fibers. For example, muscles fibers from murine models of denervation, and long-term isolated muscle fiber culturing (>5 day), exhibit changes in T-tubular morphology, such as increased number of longitudinal T-tubules,[76] abnormal Ca^{2+} signals,[33] decreased NFATc1 nuclear localization,[77] reduced NFATc1 transcriptional activity[78] and abnormal insulin signaling and glucose transporter type 4 translocation.[79] We hypothesize that hyperexcitability typical of denervated mammalian skeletal muscle,[80–82] due in part to the expression of persistent Na^+ channel currents (Nav1.5), could account for the abnormal Ca^{2+} signals observed in our results using five-day-old cultured fibers. In addition, there is evidence that denervation generally leads to altered contractile properties in both fast and slow muscles, and the re-expression of many embryonic/fetal genes.[81,83] It might be possible that elevated glucose amplifies the denervation process. Thus, further work exploring the relationship between diabetes and denervation/physical inactivity would be of interest.

Several mechanisms have been proposed as the primary event leading to abnormal Ca^{2+} signals induced by osmotic stress (i.e. tonicity-dependent dihydropyridine receptor activation, activation of mechano-sensitive channels and increased production of reactive oxygen species).[31,84,85] Regardless of the mechanism, it is clear that acute exposure to extremely elevated glucose disrupts the skeletal muscle's tubular system and triggers Ca^{2+} signals. Interestingly, it has been reported that in cerebral arterial myocytes isolated from type 2 diabetic mice, hyper-glycemia increases Ca^{2+} influx and may contribute to vascular dysfunction during diabetes.[45] The above evidence and our results suggest that abnormal Ca^{2+} signals in muscle fibers under a variety of different conditions (i.e. type 1 versus type 2 diabetes; extreme versus moderate hyperglycemia; smooth versus skeletal myocytes) may represent a common feature of the pathophysiology of diabetes and warrants further research.

There are reports that diabetic patients admitted to the emergency room with glucose levels >1000 mg/dL and diagnosed with an episode of HHS have developed rhabdomyolysis, a potentially life-threatening syndrome characterized by the breakdown of skeletal muscle, resulting in the subsequent release of intracellular contents into the circula-tory system potentially leading to renal failure.[64–66] We hypothesize that tubular system fragility and abnormal Ca^{2+} signals may be an important trigger of muscle damage in diabetic individuals undergoing an episode of HHS.

One goal of future research is to investigate the gene expression programs regulated by increasing levels of extra-cellular glucose in skeletal muscle and its potential relationship with Ca^{2+} signals and changes in tubular system morphology observed here. In particular, the use of animal models of long-term diabetes or animals displaying extreme hyperglycemia will be useful, since this might provide clues about the physiopathology of acute metabolic complications of diabetes. Overall, while the osmoprotective function of NFAT5 is best studied for its critical role in the physiologically hypertonic renal medulla, the NFAT5 pathway operates in skeletal muscle and other cell types in response to osmotic stress under certain pathologic conditions.

Acknowledgments

This work was supported by NIH-NIAMS Grants R01-AR055099 and R01-AR056477 to MFS. PR was supported by the Interdisciplinary Training Program Muscle Biology T32-AR007592. The authors thank Dr Jeffery D

Molkentin (Division of Molecular Cardiovascular Biology, Children's Hospital Medical Center) for providing the reporter 9X-NFAT-luc, and Dr William R Randall (Department of Pharmacology and Experimental Therapeutics, University of Maryland, School of Medicine) for providing the recombinant adenovirus of CMV/β-galactosidase.

REFERENCES

1. Crabtree GR, Olson EN. NFAT signaling: choreographing the social lives of cells. Cell. 2002; 109(Suppl):S67–79. [PubMed: 11983154]
2. Rao A, Luo C, Hogan PG. Transcription factors of the NFAT family: regulation and function. Annu Rev Immunol. 1997; 15:707–47. [PubMed: 9143705]
3. Lopez-Rodriguez C, Aramburu J, Rakeman AS, Rao A. NFAT5, a constitutively nuclear NFAT protein that does not cooperate with Fos and Jun. Proc Natl Acad Sci USA. 1999; 96:7214–9. [PubMed: 10377394]
4. Miyakawa H, Woo SK, Dahl SC, Handler JS, Kwon HM. Tonicity-responsive enhancer binding protein, a rel-like protein that stimulates transcription in response to hypertonicity. Proc Natl Acad Sci USA. 1999; 96:2538–42. [PubMed: 10051678]
5. Ko BC, Turck CW, Lee KW, Yang Y, Chung SS. Purification, identification, and characterization of an osmotic response element binding protein. Biochem Biophys Res Commun. 2000; 270:52–61. [PubMed: 10733904]
6. Lopez-Rodriguez C, Antos CL, Shelton JM, Richardson JA, Lin F, Novobrantseva TI, Bronson RT, Igarashi P, Rao A, Olson EN. Loss of NFAT5 results in renal atrophy and lack of tonicity-responsive gene expression. Proc Natl Acad Sci USA. 2004; 101:2392–7. [PubMed: 14983020]
7. Lam AK, Ko BC, Tam S, Morris R, Yang JY, Chung SK, Chung SS. Osmotic response element-binding protein (OREBP) is an essential regulator of the urine concentrating mechanism. J Biol Chem. 2004; 279:48048–54. [PubMed: 15347663]
8. Go WY, Liu X, Roti MA, Liu F, Ho SN. NFAT5/TonEBP mutant mice define osmotic stress as a critical feature of the lymphoid microenvironment. Proc Natl Acad Sci USA. 2004; 101:10673–8. [PubMed: 15247420]
9. Lopez-Rodriguez C, Aramburu J, Jin L, Rakeman AS, Michino M, Rao A. Bridging the NFAT and NF-kappaB families: NFAT5 dimerization regulates cytokine gene transcription in response to osmotic stress. Immunity. 2001; 15:47–58. [PubMed: 11485737]
10. Loyher ML, Mutin M, Woo SK, Kwon HM, Tappaz ML. Transcription factor tonicity-responsive enhancer-binding protein (TonEBP) which transactivates osmoprotective genes is expressed and upregulated following acute systemic hypertonicity in neurons in brain. Neuroscience. 2004; 124:89–104. [PubMed: 14960342]
11. Morancho B, Minguillon J, Molkentin JD, Lopez-Rodriguez C, Aramburu J. Analysis of the transcriptional activity of endogenous NFAT5 in primary cells using transgenic NFAT-luciferase reporter mice. BMC Mol Biol. 2008; 9:13. [PubMed: 18221508]
12. Trama J, Go WY, Ho SN. The osmoprotective function of the NFAT5 transcription factor in T cell development and activation. J Immunol. 2002; 169:5477–88. [PubMed: 12421923]
13. Gajghate S, Hiyama A, Shah M, Sakai D, Anderson DG, Shapiro IM, Risbud MV. Osmolarity and intracellular calcium regulate aquaporin2 expression through TonEBP in nucleus pulposus cells of the intervertebral disc. J Bone Miner Res. 2009; 24:992–1001. [PubMed: 19138132]
14. O'Connor RS, Mills ST, Jones KA, Ho SN, Pavlath GK. A combinatorial role for NFAT5 in both myoblast migration and differentiation during skeletal muscle myogenesis. J Cell Sci. 2007; 120:149–59. [PubMed: 17164296]
15. Ito T, Asakura K, Tougou K, Fukuda T, Kubota R, Nonen S, Fujio Y, Azuma J. Regulation of cytochrome P450 2E1 under hypertonic environment through TonEBP in human hepatocytes. Mol Pharmacol. 2007; 72:173–81. [PubMed: 17440116]
16. Maallem S, Mutin M, Kwon HM, Tappaz ML. Differential cellular distribution of tonicity-induced expression of transcription factor TonEBP in the rat brain following prolonged systemic hypertonicity. Neuroscience. 2006; 137:51–71. [PubMed: 16352399]
17. Navarro P, Chiong M, Volkwein K, Moraga F, Ocaranza MP, Jalil JE, Lim SW, Kim JA, Kwon HM, Lavandero S. Osmotically-induced genes are controlled by the transcription factor TonEBP

in cultured cardiomyocytes. Biochem Biophys Res Commun. 2008; 372:326–30. [PubMed: 18502201]

18. Aramburu J, Drews-Elger K, Estrada-Gelonch A, Minguillon J, Morancho B, Santiago V, Lopez-Rodriguez C. Regulation of the hypertonic stress response and other cellular functions by the Rel-like transcription factor NFAT5. Biochem Pharmacol. 2006; 72:1597–604. [PubMed: 16904650]
19. Lee SD, Colla E, Sheen MR, Na KY, Kwon HM. Multiple domains of TonEBP cooperate to stimulate transcription in response to hypertonicity. J Biol Chem. 2003; 278:47571–7. [PubMed: 12970349]
20. Woo SK, Lee SD, Kwon HM. TonEBP transcriptional activator in the cellular response to increased osmolality. Pflugers Arch. 2002; 444:579–85. [PubMed: 12194010]
21. Ko BC, Ruepp B, Bohren KM, Gabbay KH, Chung SS. Identification and characterization of multiple osmotic response sequences in the human aldose reductase gene. J Biol Chem. 1997; 272:16431–7. [PubMed: 9195951]
22. Nakayama Y, Peng T, Sands JM, Bagnasco SM. The TonE/TonEBP pathway mediates tonicity-responsive regulation of UT-A urea transporter expression. J Biol Chem. 2000; 275:38275–80. [PubMed: 10995747]
23. Rim JS, Atta MG, Dahl SC, Berry GT, Handler JS, Kwon HM. Transcription of the sodium/myo-inositol cotransporter gene is regulated by multiple tonicity-responsive enhancers spread over 50 kilobase pairs in the 5′-flanking region. J Biol Chem. 1998; 273:20615–21. [PubMed: 9685419]
24. Takenaka M, Preston AS, Kwon HM, Handler JS. The tonicity-sensitive element that mediates increased transcription of the betaine transporter gene in response to hypertonic stress. J Biol Chem. 1994; 269:29379–81. [PubMed: 7961914]
25. Hasler U, Jeon US, Kim JA, Mordasini D, Kwon HM, Feraille E, Martin PY. Tonicity-responsive enhancer binding protein is an essential regulator of aquaporin-2 expression in renal collecting duct principal cells. J Am Soc Nephrol. 2006; 17:1521–31. [PubMed: 16641150]
26. Woo SK, Lee SD, Na KY, Park WK, Kwon HM. TonEBP/NFAT5 stimulates transcription of HSP70 in response to hypertonicity. Mol Cell Biol. 2002; 22:5753–60. [PubMed: 12138186]
27. Kwon MS, Lim SW, Kwon HM. Hypertonic stress in the kidney: a necessary evil. Physiology (Bethesda). 2009; 24:186–91. [PubMed: 19509128]
28. Kitabchi AE, Umpierrez GE, Miles JM, Fisher JN. Hyperglycemic crises in adult patients with diabetes. Diabetes Care. 2009; 32:1335–43. [PubMed: 19564476]
29. Rosenbloom AL. Hyperglycemic hyperosmolar state: an emerging pediatric problem. J Pediatr. 2010; 156:180–4. [PubMed: 20105637]
30. Apostol S, Ursu D, Lehmann-Horn F, Melzer W. Local calcium signals induced by hyper-osmotic stress in mammalian skeletal muscle cells. J Muscle Res Cell Motil. 2009; 30:97–109. [PubMed: 19437123]
31. Pickering JD, White E, Duke AM, Steele DS. DHPR activation underlies SR Ca2+ release induced by osmotic stress in isolated rat skeletal muscle fibers. J Gen Physiol. 2009; 133:511–24. [PubMed: 19398777]
32. Wang X, Weisleder N, Collet C, Zhou J, Chu Y, Hirata Y, Zhao X, Pan Z, Brotto M, Cheng H, Ma J. Uncontrolled calcium sparks act as a dystrophic signal for mammalian skeletal muscle. Nat Cell Biol. 2005; 7:525–30. [PubMed: 15834406]
33. Brown LD, Rodney GG, Hernandez-Ochoa E, Ward CW, Schneider MF. Ca2+ sparks and T tubule reorganization in dedifferentiating adult mouse skeletal muscle fibers. Am J Physiol Cell Physiol. 2007; 292:C1156–66. [PubMed: 17065203]
34. Liu Y, Carroll SL, Klein MG, Schneider MF. Calcium transients and calcium homeostasis in adult mouse fast-twitch skeletal muscle fibers in culture. Am J Physiol. 1997; 272:C1919–27. [PubMed: 9227421]
35. Liu Y, Cseresnyes Z, Randall WR, Schneider MF. Activity-dependent nuclear translocation and intranuclear distribution of NFATc in adult skeletal muscle fibers. J Cell Biol. 2001; 155:27–39. [PubMed: 11581284]
36. Brown LD, Schneider MF. Delayed dedifferentiation and retention of properties in dissociated adult skeletal muscle fibers in vitro. In Vitro Cell Dev Biol Anim. 2002; 38:411–22. [PubMed: 12534341]

37. Yang P, Zhao Z, Reece EA. Involvement of c-Jun N-terminal kinases activation in diabetic embryopathy. Biochem Biophys Res Commun. 2007; 357:749–54. [PubMed: 17449011]
38. Wilkins BJ, Dai YS, Bueno OF, Parsons SA, Xu J, Plank DM, Jones F, Kimball TR, Molkentin JD. Calcineurin/NFAT coupling participates in pathological, but not physiological, cardiac hypertrophy. Circ Res. 2004; 94:110–8. [PubMed: 14656927]
39. Prosser BL, Hernandez-Ochoa E, Lovering RM, Andronache Z, Zimmer DB, Melzer W, Schneider MF. S100A1 promotes action potential-initiated calcium release flux and force production in skeletal muscle. Am J Physiol Cell Physiol. 2010; 299:C891–902. [PubMed: 20686070]
40. Prosser BL, Wright NT, Hernandez-Ochoa EO, Varney KM, Liu Y, Olojo RO, Zimmer DB, Weber DJ, Schneider MF. S100A1 binds to the calmodulin-binding site of ryanodine receptor and modulates skeletal muscle excitation-contraction coupling. J Biol Chem. 2008; 283:5046–57. [PubMed: 18089560]
41. Grynkiewicz G, Poenie M, Tsien RY. A new generation of Ca2+ indicators with greatly improved fluorescence properties. J Biol Chem. 1985; 260:3440–50. [PubMed: 3838314]
42. Zhou J, Yi J, Royer L, Launikonis BS, Gonzalez A, Garcia J, Rios E. A probable role of dihydropyridine receptors in repression of Ca2+ sparks demonstrated in cultured mammalian muscle. Am J Physiol Cell Physiol. 2006; 290:C539–53. [PubMed: 16148029]
43. Chonkar A, Hopkin R, Adeghate E, Singh J. Contraction and cation contents of skeletal soleus and EDL muscles in age-matched control and diabetic rats. Ann N Y Acad Sci. 2006; 1084:442–51. [PubMed: 17151321]
44. McGuire M, MacDermott M. The influence of streptozotocin diabetes and metformin on erythrocyte volume and on the membrane potential and the contractile characteristics of the extensor digitorum longus and soleus muscles in rats. Exp Physiol. 1999; 84:1051–8. [PubMed: 10564702]
45. Navedo MF, Takeda Y, Nieves-Cintron M, Molkentin JD, Santana LF. Elevated Ca^{2+} sparklet activity during acute hyperglycemia and diabetes in cerebral arterial smooth muscle cells. Am J Physiol Cell Physiol. 2010; 298:C211–20. [PubMed: 19846755]
46. van Lunteren E, Moyer M. Altered diaphragm muscle action potentials in Zucker diabetic fatty (ZDF) rats. Respir Physiol Neurobiol. 2006; 153:157–65. [PubMed: 16311078]
47. Kratz A, Ferraro M, Sluss PM, Lewandrowski KB. Case records of the Massachusetts General Hospital. Weekly clinicopathological exercises. Laboratory reference values. *N Engl J* Med. 2004; 351:1548–63. [PubMed: 15470219]
48. Ferraris JD, Persaud P, Williams CK, Chen Y, Burg MB. cAMP-independent role of PKA in tonicity-induced transactivation of tonicity-responsive enhancer/ osmotic response element-binding protein. Proc Natl Acad Sci USA. 2002; 99:16800–5. [PubMed: 12482947]
49. Irarrazabal CE, Liu JC, Burg MB, Ferraris JD. ATM, a DNA damage-inducible kinase, contributes to activation by high NaCl of the transcription factor TonEBP/OREBP. Proc Natl Acad Sci USA. 2004; 101:8809–14. [PubMed: 15173573]
50. Ko BC, Lam AK, Kapus A, Fan L, Chung SK, Chung SS. Fyn and p38 signaling are both required for maximal hypertonic activation of the osmotic response element-binding protein/tonicity-responsive enhancer-binding protein (OREBP/TonEBP). J Biol Chem. 2002; 277:46085–92. [PubMed: 12359721]
51. Tsai TT, Guttapalli A, Agrawal A, Albert TJ, Shapiro IM, Risbud MV. MEK/ERK signaling controls osmoregulation of nucleus pulposus cells of the intervertebral disc by transactivation of TonEBP/OREBP. J Bone Miner Res. 2007; 22:965–74. [PubMed: 17371162]
52. Zhou X, Ferraris JD, Dmitrieva NI, Liu Y, Burg MB. MKP-1 inhibits high NaCl-induced activation of p38 but does not inhibit the activation of TonEBP/OREBP: opposite roles of p38alpha and p38delta. Proc Natl Acad Sci USA. 2008; 105:5620–5. [PubMed: 18367666]
53. Irarrazabal CE, Burg MB, Ward SG, Ferraris JD. Phosphatidylinositol 3-kinase mediates activation of ATM by high NaCl and by ionizing radiation: role in osmoprotective transcriptional regulation. Proc Natl Acad Sci USA. 2006; 103:8882–7. [PubMed: 16728507]
54. Irarrazabal CE, Gallazzini M, Schnetz MP, Kunin M, Simons BL, Williams CK, Burg MB, Ferraris JD. Phospholipase C-gamma1 is involved in signaling the activation by high NaCl of the

osmoprotective transcription factor TonEBP/OREBP. Proc Natl Acad Sci USA. 2010; 107:906–11. [PubMed: 20080774]

55. Zhou X, Gallazzini M, Burg MB, Ferraris JD. Contribution of SHP-1 protein tyrosine phosphatase to osmotic regulation of the transcription factor TonEBP/OREBP. Proc Natl Acad Sci USA. 2010; 107:7072–7. [PubMed: 20351292]
56. Aramburu J, Lopez-Rodriguez C. Brx shines a light on the route from hyperosmolarity to NFAT5. Sci Signal. 2009; 2:pe20. [PubMed: 19351952]
57. Clark KA, McElhinny AS, Beckerle MC, Gregorio CC. Striated muscle cytoarchitecture: an intricate web of form and function. Annu Rev Cell Dev Biol. 2002; 18:637–706. [PubMed: 12142273]
58. Peachey LD. The sarcoplasmic reticulum and transverse tubules of the frog's sartorius. J Cell Biol. 1965; 25(Suppl.):209–31. [PubMed: 5840799]
59. Franzini-Armstrong C, Porter KR. Sarcolemmal invaginations constituting the T system in fish muscle fibers. J Cell Biol. 1964; 22:675–96. [PubMed: 14208357]
60. Franzini-Armstrong C, Jorgensen AO. Structure and development of E-C coupling units in skeletal muscle. Ann Rev Physiol. 1994; 56:509–34. [PubMed: 8010750]
61. Shen T, Liu Y, Contreras M, Hernandez-Ochoa EO, Randall WR, Schneider MF. DNA binding sites target nuclear NFATc1 to heterochromatin regions in adult skeletal muscle fibers. Histochem Cell Biol. 2010; 134:387–402. [PubMed: 20865272]
62. Chen S, Grigsby CL, Law CS, Ni X, Nekrep N, Olsen K, Humphreys MH, Gardner DG. Tonicity-dependent induction of Sgk1 expression has a potential role in dehydration-induced natriuresis in rodents. J Clin Invest. 2009; 119:1647–58. [PubMed: 19436108]
63. Bain J, Plater L, Elliott M, Shpiro N, Hastie CJ, McLauchlan H, Klevernic I, Arthur JS, Alessi DR, Cohen P. The selectivity of protein kinase inhibitors: a further update. Biochem J. 2007; 408:297–315. [PubMed: 17850214]
64. Baluch AR, Oommen SP. Malignant hyperthermia associated with diabetic hyperosmolar hyperglycemic nonketotic state in a young man. J Clin Anesth. 2007; 19:470–2. [PubMed: 17967680]
65. Gangopadhyay KK, Ryder RE. Nontraumatic rhabdomyolysis: an unusual complication of diabetic hyperosmolar nonketotic (HONK) state. J R Soc Med. 2006; 99:200. [PubMed: 16574974]
66. Ka T, Takahashi S, Tsutsumi Z, Moriwaki Y, Yamamoto T, Fukuchi M. Hyperosmolar non-ketotic diabetic syndrome associated with rhabdomyolysis and acute renal failure: a case report and review of literature. Diabetes Nutr Metab. 2003; 16:317–22. [PubMed: 15000444]
67. Eisenberg RS, Gage PW. Frog skeletal muscle fibers: changes in electrical properties after disruption of transverse tubular system. Science. 1967; 158:1700–1. [PubMed: 6070028]
68. Howell JN. A lesion of the transverse tubules of skeletal muscle. J Physiol. 1969; 201:515–33. [PubMed: 5767880]
69. Eisenberg B, Eisenberg RS. Transverse tubular system in glycerol-treated skeletal muscle. Science. 1968; 160:1243–4. [PubMed: 5648264]
70. Caputo C. Volume and twitch tension changes in single muscle fibers in hypertonic solutions. J Gen Physiol. 1968; 52:793–809. [PubMed: 5688084]
71. Peachey, LD.; Francini-Armstrong, C. Structure and function of membrane systems of skeletal muscle cells. In: Peachey, LD., editor. Handbook of Physiology, Section 10: Skeletal muscle. American Physiological Society; Bethesda, MD: 1983. p. 23-71.
72. Beam, KG.; Horowicz, P. Excitation–contraction coupling in skeletal muscle. 3th edn. Engel, AG.; Franzini-Armstrong, C., editors. McGraw-Hill; New York: 2004.
73. Veratti E. Investigations on the fine structure of striated muscle fiber read before the Reale Istituto Lombardo, 13 March 1902. J Biophys Biochem Cytol. 1961; 10(Suppl):1–59. [PubMed: 13780770]
74. Edwards JN, Launikonis BS. The accessibility and interconnectivity of the tubular system network in toad skeletal muscle. J Physiol. 2008; 586:5077–89. [PubMed: 18772207]
75. Edwards JN, Cully TR, Shannon TR, Stephenson DG, Launikonis BS. Longitudinal and transversal propagation of excitation along the tubular system of rat fast-twitch muscle fibres studied by high speed confocal microscopy. J Physiol. 2011; 590:475–92. [PubMed: 22155929]

76. Takekura H, Tamaki H, Nishizawa T, Kasuga N. Plasticity of the transverse tubules following denervation and subsequent reinnervation in rat slow and fast muscle fibres. J Muscle Res Cell Motil. 2003; 24:439–51. [PubMed: 14677647]

77. Tothova J, Blaauw B, Pallafacchina G, Rudolf R, Argentini C, Reggiani C, Schiaffino S. NFATc1 nucleocytoplasmic shuttling is controlled by nerve activity in skeletal muscle. J Cell Sci. 2006; 119:1604–11. [PubMed: 16569660]

78. McCullagh KJ, Calabria E, Pallafacchina G, Ciciliot S, Serrano AL, Argentini C, Kalhovde JM, Lømo T, Schiaffino S. NFAT is a nerve activity sensor in skeletal muscle and controls activity-dependent myosin switching. Proc Natl Acad Sci USA. 2004; 101:10590–5. [PubMed: 15247427]

79. Lauritzen HP, Ploug T, Ai H, Donsmark M, Prats C, Galbo H. Denervation and high-fat diet reduce insulin signaling in T-tubules in skeletal muscle of living mice. Diabetes. 2008; 57:13–23. [PubMed: 17914033]

80. Ware F Jr. Bennett AL, Mc IA. Membrane resting potential of denervated mammalian skeletal muscle measured *in vivo*. Am J Physiol. 1954; 177:115–8. [PubMed: 13148353]

81. Midrio M. The denervated muscle: facts and hypotheses. A historical review. Eur J Appl Physiol. 2006; 98:1–21. [PubMed: 16896733]

82. Purves D, Sakmann B. Membrane properties underlying spontaneous activity of denervated muscle fibres. J Physiol. 1974; 239:125–53. [PubMed: 4853156]

83. Rana ZA, Gundersen K, Buonanno A. The ups and downs of gene regulation by electrical activity in skeletal muscles. J Muscle Res Cell Motil. 2009; 30:255–60. [PubMed: 20135341]

84. Teichmann MD, Wegner FV, Fink RH, Chamberlain JS, Launikonis BS, Martinac B, Friedrich O. Inhibitory control over Ca(2+) sparks via mechanosensitive channels is disrupted in dystrophin deficient muscle but restored by mini-dystrophin expression. PLoS One. 2008; 3:e3644. [PubMed: 18982068]

85. Martins AS, Shkryl VM, Nowycky MC, Shirokova N. Reactive oxygen species contribute to Ca2+ signals produced by osmotic stress in mouse skeletal muscle fibres. J Physiol. 2008; 586:197–210. [PubMed: 17974587]

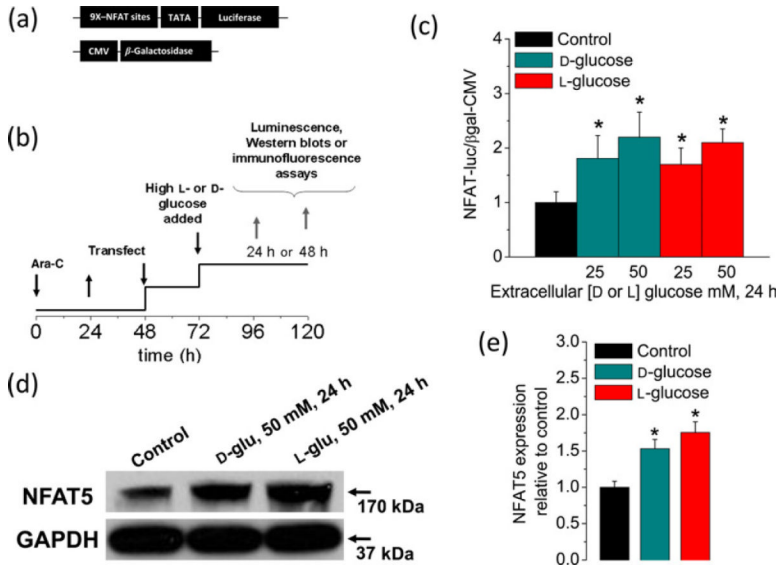

Figure 1.

Sustained elevation in extracellular glucose enhances NFAT-dependent transcriptional activity and NFAT5 expression. (a) Schematic representation of the reporters used in this study. (b) Protocol used for experiments illustrated also in Figures 2–5. After plating, FDB fibers were treated with ara-C for 24 h, then ara-C was washed out. Then, after 48 h, plated fibers were co-transfected with adenovirus containing NFAT-driven luciferase and CMV-driven β-galactosidase reporters. Transfection was not performed in fibers used for Western blot and immunofluorescence assays. Beginning one day after transfection, fibers were maintained in control and isotonic (5.56 mmol/L D-glucose; 288 mOsm/kg) media or in high D-or L-glucose medium (25–50 mmol/L; 308–336 mOsm/kg) for 24–48 h. After this time, cells were homogenated and assayed for luciferase and β-galactosidase activities or Western blot. (c) NFAT-dependent transcriptional activity was enhanced by increasing D-or L-glucose concentrations (for 24 h). Mean ± SE of four independent experiments (four mice per group) are shown. (d) Western blot analysis of whole-cell homogenates prepared from FDB fibers cultured in control isotonic media or in high D-or L-glucose (50 mmol/L) media for 24 h by using NFAT5 antibody. The blot is representative of three independent experiments (three mice per group). (e) Quantification of Western blotdata indicates a substantial increase of NFAT5 expression by elevated D-or L-glucose. *Indicates $P< 0.05$ compared with control. NFAT, nuclear factor of activated T-cell; FDB, *flexor digitorum brevis*; ara-C, cytosine β-D-arabinofuranoside; CMV cytomegalovirus; GAPDH, glyceraldehyde-3-phosphate dehydrogenase. (A color version of this figure is available in the online journal)

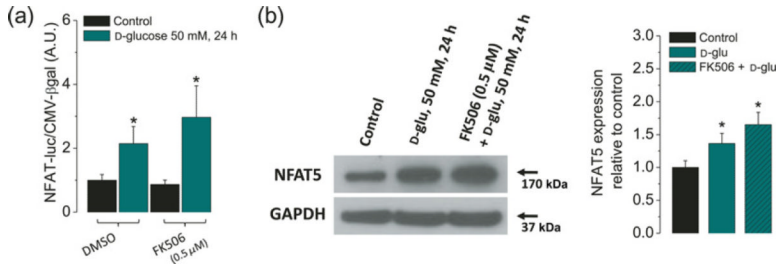

Figure 2.

High glucose-dependent activation of the NFAT-luciferase reporter and NFAT5 expression are insensitive to the calcineurin-A inhibitor FK506. Fibers were transfected as in the protocol indicated in Figure 1a. One day after transfection, fibers were transferred to isotonic or high-glucose (50 mmol/L) media with DMSO (0.5% v/v) or with FK506 (0.5 μmol/L), a calcineurin-A inhibitor, during 24 h. (a) Luciferase activity driven by NFAT normalized to β-galactosidase activity driven by CMV relative to control fibers. Mean ± S.E. of four independent experiments (four mice per group) is shown. (b) Western blot analysis of whole cell homogenates prepared from FDB fibers cultured in control isotonic media or in high D-glucose (50 mmol/L) media with DMSO (0.5% v/v) or with FK506 (0.5 μmol/L) for 24 h by using NFAT5 antibody. The blot is representative of three independent experiments (three mice per group). The bar plot is the result of triplicate experiments, showing that the increase on NFAT5 expression induced by elevated glucose is insensitive to the calcineurin-A inhibitor FK506. *Indicates $P < 0.05$ compared with control. NFAT, nuclear factor of activated T-cell; DMSO, dimethyl sulfoxide; CMV, cytomegalovirus; FDB, *flexor digitorum brevis*; GAPDH, glyceraldehyde-3-phosphate dehydrogenase. (A color version of this figure is available in the online journal)

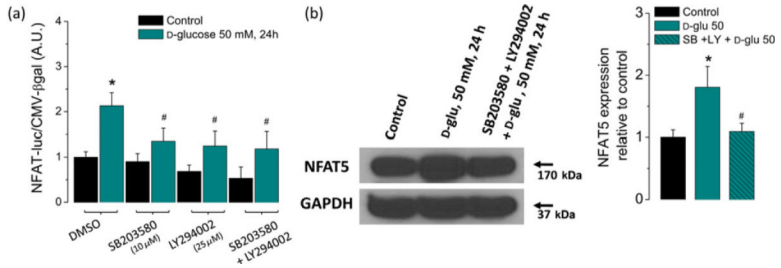

Figure 3.

High glucose-dependent activation of the NFAT-luciferase reporter and NFAT5 expression are sensitive to inhibitors of stress kinases p38α and PIKK. FDB fibers were transfected as in Figure 1a. One day after transfection, fibers were transferred to isotonic or high-glucose (50 mmol/L) media with DMSO (0.5% v/v) or with SB203580 (10 μmol/L; a p38α inhibitor), LY2940002 (25 μmol/L; a PIKK inhibitor) or both (SB203580 + LY2940002) during 24 h. (a) Luciferase activity driven by NFAT normalized to β-galactosidase activity driven by CMV relative to control fibers. Mean ± S.E of three independent experiments is shown. (b) Western blot analysis of whole cell homogenates prepared from FDB fibers cultured in control isotonic media or in high D-glucose (50 mmol/L) media with DMSO (0.5% v/v) or with the combination of SB203580 + LY2940002 for 24 h by using NFAT5 antibody. The blot is representative of three independent experiments (three mice per group). The bar plot indicates that the increase on NFAT5 expression induced by elevated glucose is sensitive to inhibitors of stress kinases p38α and PIKK. *Indicates $P < 0.05$ compared with control; $^{\#}P < 0.05$ compared with fibers exposed to D-glucose without inhibitors. NFAT, nuclear factor of activated T-cell; DMSO, dimethyl sulfoxide; FDB, *flexor digitorum brevis*; PIKK, phosphoinositide 3-kinase-related kinase; CMV, cytomegalovirus; GAPDH, glyceraldehyde-3-phosphate dehydrogenase. (A color version of this figure is available in the online journal)

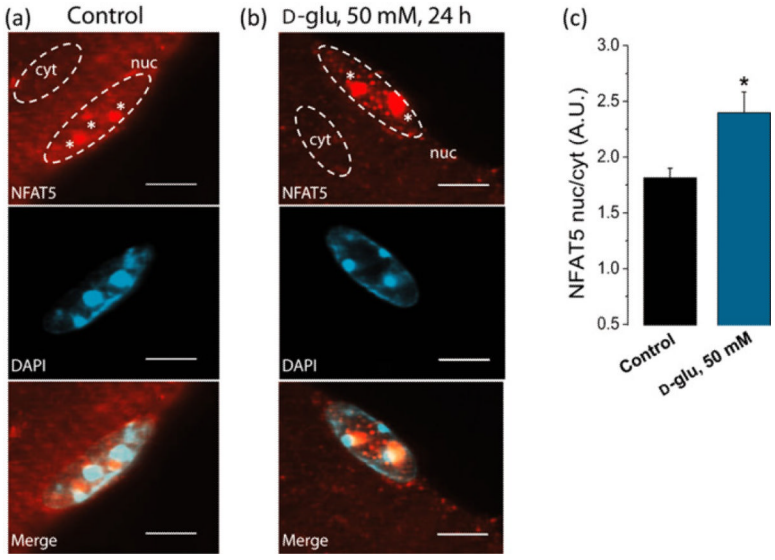

Figure 4.

Sustained elevation in extracellular glucose enhances NFAT5 nuclear translocation. Following the protocol described in Figure 1a, at 72 h after plating, fibers were transferred to isotonic or high D-glucose medium for 24 h; after this time, cells were fixed and assayed by immunofluorescence using a monoclonal NFAT5 antibody. (a and b) Representation of confocal images illustrating the distribution of NFAT5 (top panels) and DAPI staining (middle panels) in FDB fibers exposed to isotonic (a) or elevated (50 mmol/L) D-glucose (b). Merged images are shown in bottom panels. Asterisks in top panels (a) and (b) indicate a distinct pattern of fluorescent foci (1–3 foci per nucleus of about 1–3 μm in diameter). Scale bar: 5 μm. (c) Quantification of average nuclear translocation in control (n = 14 fibers, three mice) and D-glucose-exposed fibers (n = 14 fibers, three mice), measured as the ratio of nuclear/cytosolic NFAT5-Alexa-488 fluorescence measured in the regions of interest illustrated in (a) and (b). *Indicates $P < 0.05$ compared with control. NFAT5, nuclear factor of activated T-cell; DAPI, 4',6-diamidino-2-phenylindole; FDB, *flexor digitorum brevis*. (A color version of this figure is available in the online journal)

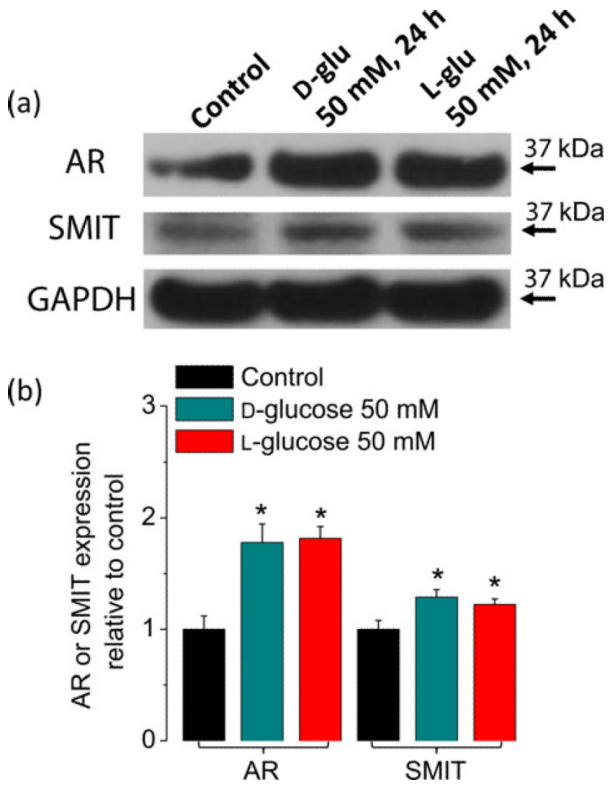

Figure 5.

Activation of NFAT5-dependent osmoprotective genes after an elevation in extracellular D-glucose. (a) Western blot analysis of whole-cell homogenates prepared from FDB fibers cultured in control isotonic or in elevated extracellular D-glucose (50 mmol/L) media for 24 h using AR, SMIT and GAPDH antibodies. The blots are representative of three independent experiments (three mice per group). (b) Quantification of Western blot data indicates a substantial increase of AR and a more modest increase of SMIT by elevated D-glucose. Data are the mean ± SE. *Indicates $P < 0.05$ compared with control. NFAT5, nuclear factor of activated T-cells 5; FDB, *flexor digitorum brevis*; AR, aldose reductase; SMIT, sodium/myo-inositol transporter; GAPDH, glyceraldehyde-3-phosphate dehydrogenase. (A color version of this figure is available in the online journal)

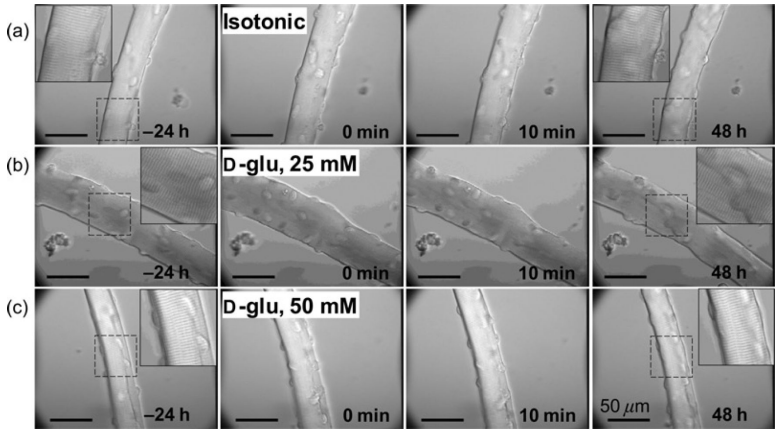

Figure 6.

Fibers exposed to elevated glucose do not exhibit major changes in gross morphology. Representative differential interference contrast microscopy images from a 72-h time-lapse experiment from a control fiber maintained in isotonic control (5.56 mmol/L D-glucose) media (a), from another fiber treated with 25 mmol/L added D-glucose (b) and from another fiber treated with 50 mmol/L added D-glucose (c). Isotonic or elevated glucose-containing media changes were conducted at time 0. Scale bars: 50 μm. Fibers (10–14 fibers, three mice per condition) were able to resist the treatment with elevated glucose for up to 48 h without displaying any major disturbance in morphology

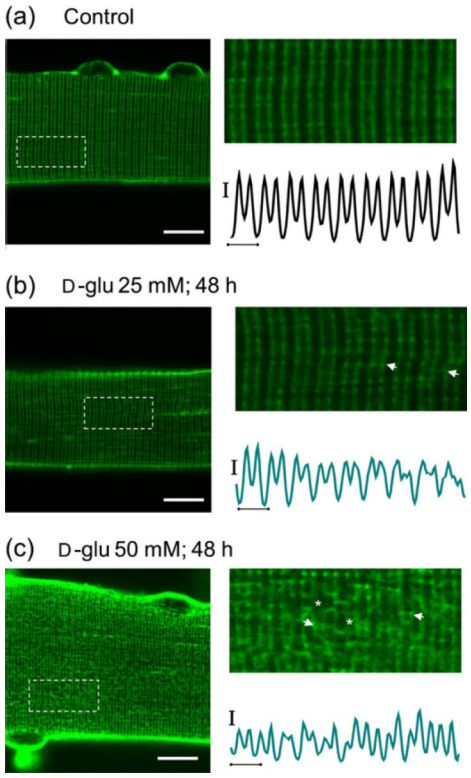

Figure 7.

Transverse tubular system disruption accompanying D-glucose exposure. Confocal images of FDB muscle fibers maintained in isotonic control (5.56 mmol/L D-glucose) medium (a) (n = 22 fibers, three mice), 25 mmol/L D-glucose (b) (n = 36 fibers, three mice) and 50 mmol/L (c) (n = 28 fibers, three mice) for 48 h and then stained with di-8-ANEPPS (see protocol in Figure 9a). Scale bars: 10 μm. (a–c) Right panels, zoom-in versions of boxed regions indicated in left panels. Traces below zoom-in images are averaged fluorescence profiles across the box, vertical scale bar: 500 A.U.; horizontal scale bar: 2 μm. Di-8-ANEPPS staining reveals that the normally regular transverse-tubule morphology (a) is moderately affected in fibers exposed to 25 mmol/L D-glucose for 48 h (b), but is remarkably disrupted in fibers exposed to 50 mmol/L D-glucose for 48 h (c). The asterisks indicate places of transverse tubule dilation and the arrows indicate locations where adjacent transverse tubule appear to make close contact. FDB, *flexor digitorum brevis*; NFAT5, nuclear factor of activated T-cells 5; A.U., arbitrary units. (A color version of this figure is available in the online journal)

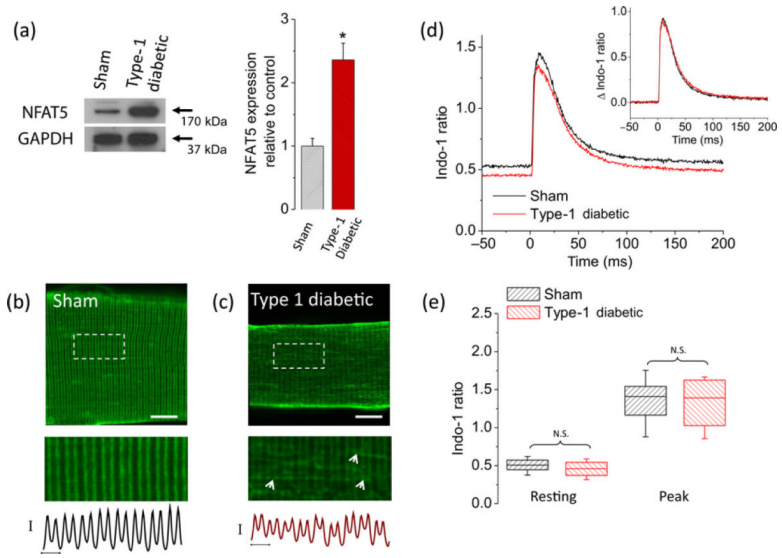

Figure 8.

Fibers from type 1 diabetic mice display an increase in NFAT5 expression and transverse tubule system disruption but no changes in electrically evoked Ca^{2+} transients. (a) Left, Western blot analysis of whole cell homogenates prepared from TA muscles from sham, non-diabetic mice or from type 1 diabetic mice. The blot is representative of three independent experiments, three mice per condition. Right, quantification of Western blot data indicates a substantial increase of NFAT5 expression in type 1 diabetic mice. *Indicates $P < 0.05$ compared with sham, non-diabetic control. Representative confocal images of the transverse tubule morphology of FDB fibers isolated from sham, non-diabetic (b) ($n = 30$ fibers, four mice) and type 1 diabetic mice (c) ($n = 30$ fibers, four mice) and stained with di-8-ANEPPS. Scale bar: 20 μm. Bottom images are zoom-in versions of boxed regions indicated in panels (b) and (c). Traces below zoom-in images are averaged fluorescence profiles across the box, vertical scale bar: 500 A.U.; horizontal scale bar: 2 μm. Di-8-ANEPPS staining reveals that transverse tubule morphology is disrupted in fibers from diabetic mice. (d) Time course of electrically evoked Ca^{2+} transients, using the Ca^{2+} indicator indo-1, from single muscle fibers from sham, non-diabetic mice (black trace; $n = 31$ fibers, four mice) and from type 1 diabetic mice (red trace; $n = 35$ fibers, four mice). Inset, Δ indo-1 ratio (Δ indo-1 ratio = (indo-1 ratio) – (resting indo-1 ratio)), shows negligible differences in the amplitude and kinetics of electrically evoked Ca^{2+} transients from fibers isolated from type 1 diabetic mice when compared with sham, non-diabetic counterparts. (e) Box-plot summary of indo-1 ratio measurements at rest and peak; median indo-1 ratio values are shown by solid lines within each box on distribution plots. Box upper and lower limits represent the 75th and 25th percentiles, respectively; the extended lines indicate the 10th and 90th percentiles. No significant changes in resting or peak indo-1 ratio values were found in fibers from type 1 diabetic mice when compared with control counterparts. For experiments using FDB fibers from diabetic mice in panels (b)–(e), glucose in media was maintained at the same levels as found *in vivo* (average plasma glucose in type 1 diabetic mice was 22 mmol/L). One day after plating, FDB fibers from type 1 diabetic mice and sham, non-diabetic mice were stained with Di-8-ANEPPS or loaded with indo-1 AM (see Materials and methods) and then resting ratio and electrically evoked Ca^{2+} transients were measured. N.S., not significant; A.U., arbitrary units; NFAT5, nuclear factor of activated T-cells 5; FDB, *flexor digitorum brevis*; TA, tibialis anterior; GAPDH, glyceraldehyde-3-phosphate dehydrogenase. (A color version of this figure is available in the online journal)

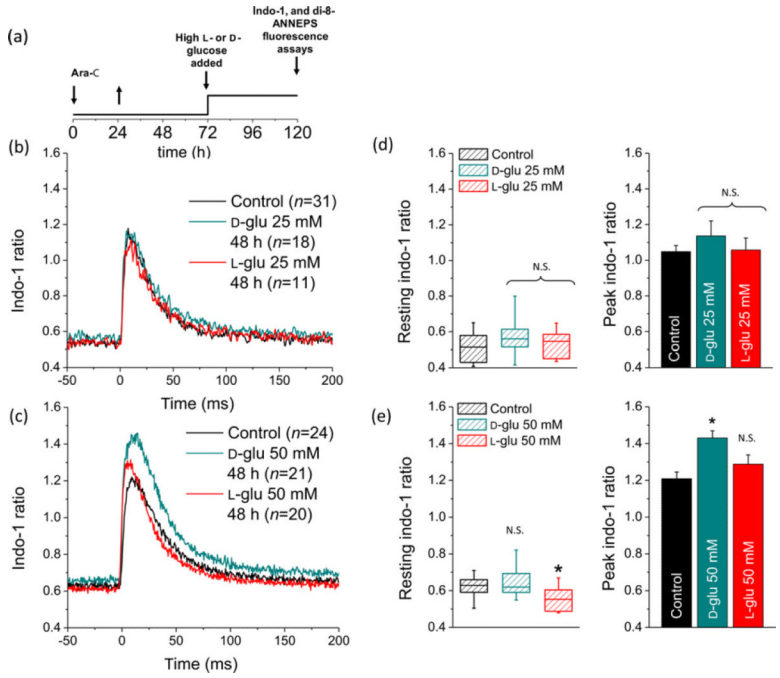

Figure 9.

Sustained elevated D-glucose enhances electrically evoked Ca^{2+} transients. (a) Time course of the experiments using di-8-ANEPPS and indo-1, also in Figure 7. After plating, FDB fibers were treated with ara-C for 24 h, then ara-C was washed out. Then, three days after plating, fibers were maintained in control isotonic (5.56 mmol/L D-glucose; 288 mOsm/kg) or in high D- or L-glucose (25–50 mmol/L; osmolality 308–336 mOsm/kg) medium for 24–48 h; after this time, cells were loaded/stained with Ca^{2+} indicator or with di-8-ANEPPS. (b) Time course of electrically evoked indo-1 transients in fibers maintained in control media (black trace; $n = 31$ fibers, six mice), 25 mmol/L D-glucose (cyan trace, $n = 18$ fibers, six mice) or 25 mmol/L L-glucose (red trace, $n = 11$ fibers, five mice). (c) Time course of electrically evoked indo-1 transients in fibers maintained in control media (black trace; $n = 24$ fibers, six mice), 50 mmol/L D-glucose (cyan trace; $n = 21$ fibers, eight mice) or 50 mmol/L L-glucose (red trace; $n = 20$ fibers, six mice) for 48 h. (d) Summary of rest and at peak indo-1 ratio measurements for fibers exposed to 25 mmol/L elevated glucose. (e) Summary of rest and at peak indo-1 ratio measurements for fibers exposed to 50 mmol/L elevated glucose. No significant changes in resting indo-1 ratio were found in fibers challenged with either 25 mmol/L (d, *left*) or 50 mmol/L (e, *left*) elevated D-glucose. L-glucose at 50 mmol/L induced a small but significant reduction in resting indo-1 ratio (e, *left*). In box plots, median indo-1 ratio values are shown by solid lines within each box, upper and lower limits represent the 75th and 25th percentiles, respectively; the extended lines indicate the 10th and 90th percentiles. No significant changes in peak indo-1 ratio were found in fibers challenged with 25 mmol/L D-or L-glucose-exposed fibers (d, *right*). Fibers exposed to 50 mmol/L D-glucose displayed a significantly larger action potential-induced Ca^{2+} transient (e, *right*). *Indicates $P < 0.05$ compared with control. N.S. not significant; FDB, *flexor digitorum brevis*; ara-C, cytosine β-D-arabinofuranoside. (A color version of this figure is available in the online journal)